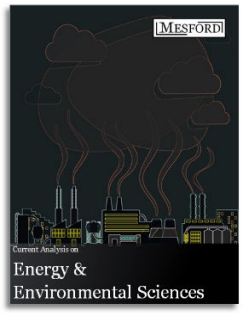

Compact Fixed-bed Chemical Looping Combustion Process for Power Generation with Near Zero CO_2 Emissions

José Ramón Fernández*

Spanish Research Council, INCAR-CSIC. C/ Francisco Pintado Fe, 26, 33011, Oviedo, Spain.

Abstract:

A process scheme based on fixed-bed reactors is presented as a possible alternative for carrying out the chemical looping combustion of methane at high pressure with gas recycles suitable for controlling the gradients of temperature in the beds. This process is designed to exploit the advantages of the Ni/NiO redox system for chemical looping combustion applications by providing a good reactivity, a high O_2 carrying capacity and also chemical and thermal stability. The oxygen carrier, which is stationary, is alternately exposed to reducing and oxidizing atmospheres by means of the periodic switching of the gas feeds (fuel gas and air, respectively). Simple reactor models designed to quantify the temperature profiles during the reaction stages of the process reveal that the increase in temperature in the Ni oxidation fronts can be moderated by introducing cooled nitrogen recycles into the oxidation stages of the process. In these conditions, oxygen carriers with a higher Ni content (around 60 wt.%) can be used, to allow more compact reactor designs. Moreover, the ability to control the displacement of the reaction and heat exchange fronts enables the reduction stage to be initiated with a lower fraction of solids at high temperature. Consequently, a larger proportion of the heat generated during the Ni oxidation stages can be used for power generation by expanding the high temperature pressurized N_2 in a gas turbine. A sequence of five stages is shown to be necessary to facilitate the redox reactions and satisfy the energy requirements of the process. The basic design an the thermal integration of this configuration for 10 kg/s of methane (around 500 MWth) is discussed and reasonable operating conditions for the reactors are proposed. A minimum duration of about 10 minutes is considered to be sufficient time for each stage of the CLC process to be completed. A minimum L/D ratio of about 1.7 and a maximum pressure drop of about 10% are assumed for the process to be successfully carried out using 6 reactors, 7 m long with an inner diameter of 4 m. About 55% of energy efficiency with 98% of CO_2 capture efficiency have been calculated, which means only 3.5 points of energy penalty compared to a natural gas combined cycle without CO_2 capture. These results confirm the potential of this novel process as a future power generation system with near zero CO_2 emissions.

Publication History: Received: 01 November 2018 | Revised: 08 March 2019 |Accepted: 11 March 2019

Keywords:
CO_2 capture; chemical looping combustion; fixed-bed reactors; nickel; methane; thermal integration

1. INTRODUCTION

The increase in anthropogenic CO_2 emissions is widely recognized as one of the main factors of global warming [1]. The expected increase in world energy demand over the next decades makes it necessary to develop urgent measures aimed at reducing greenhouse gas emissions [2]. Of the different strategies proposed to mitigate CO_2 emissions, carbon capture and storage (CCS) is considered as a valid mid-term solution [3]. However, CO_2 capture is nowadays an energy intensive process, and as a result, most of the research on CCS is directed at developing new CO_2 capture technologies with minimum energy penalties and lower equipment cost [4, 5]. Chemical looping combustion (CLC) is an emerging technology, which consists in the transfer of oxygen from air to the fuel using a solid metal (oxygen carrier), avoiding the direct contact between the fuel and air [6-8]. The dilution of the combustion products with nitrogen is avoided and the product gas is highly concentrated in CO_2, as it happens in oxy-combustion systems but without the need of a parasitic consumption to produce cryogenic O_2. While the metal oxidation reaction is always exothermic, its reduction can either be exothermic or endothermic, depending on the metal and the fuel involved. In all the cases, the heat generated by both oxidation/reduction reactions is equal to the heat of the combustion of the fuel [9, 10]. Chemical looping combustion processes are mainly intended to be carried out with configurations based on interconnected fluidized-bed reactors

*Address correspondence to this author at Spanish Research Council, INCAR-CSIC. C/ Francisco Pintado Fe, 26, 33011, Oviedo, Spain; Phone: +34 985119090, Fax: +34 985 29 76 62; E-mail: jramon@incar.csic.es

Mesford Publisher Inc
Office Address: Suite 2205, 350 Webb Drive, Mississauga, ON L5B3W4, Canada; T: +1 (647) 7109849 | E: caee@mesford.ca, contact@mesford.ca, https://mesford.ca/journals/caee/

[11-16]. This facilitates the transport of the oxygen carrier to the fuel reactor and its subsequent regeneration in the air reactor. In fluidized beds, the small size of the particles of the oxygen carrier allows a good solid/gas contact, which enhances the overall kinetics of the reactions involved in the process. Moreover, the rapid mixing of the solids in fluidized beds makes it easier to control the temperature, which is essential in chemical looping processes, where the reactions are usually highly exothermic or endothermic. However, the use of interconnected fluidized bed technology for CLC does have drawbacks for some applications. In the case of high-quality fuels like natural gas, the current reference systems for power generation (without CO_2 capture) are highly efficient combined cycles (with net efficiencies close to 0.6), which operate at high pressure. Therefore, the theoretical benefits of CLC can only be achieved when the interconnected fuel and air reactors perform at high temperatures and high pressures [17-19]. Moreover, high-temperature and high-pressure solids filtering systems are required to separate the fines resulting from the attrition of particles in the beds. The presence of fines in the flue gas streams must be avoided in order to protect the downstream gas turbine and also to reduce the potential risks to human health and the environment caused by the emissions of some oxygen carriers, such as Ni or Co [20]. Although several works based on CLC performed in interconnected fluidized beds at high pressure have been published in recent years [21, 22], this concept is still in need of further experimental validation in order to demonstrate its feasibility on a large scale. Nickel-based materials have been widely studied because of their favorable characteristics for chemical looping applications with natural gas. Apart from their high reactivity and reversibility at temperatures up to 1200 ºC, they present a very high oxygen carrying capacity and they are not hampered by thermodynamic restrictions that impede the near complete conversion of methane to CO_2 and H_2O [23, 24]. Moreover, Ni-based carriers maintain a good chemical and mechanical stability over multiple oxidation/reduction cycles, which is of great importance in processes where the replacement of particles can be costly [25, 26].

CLC processes can be implemented in configurations based on packed-bed reactor technology that has been proposed as an alternative for power generation with a high level of energy efficiency [27, 28]. In this case, the oxygen carrier remains stationary and it is alternately exposed to reducing and oxidizing atmospheres by means of the periodic switching of the gas stream fed into the system (fuel gas and air, respectively). By operating several reactors in parallel, a continuous high-temperature and high-pressure gas stream is produced and used to drive a gas turbine (see Fig. **1**). In contrast to fluidized-bed configurations, operational problems arising from the attrition of the oxygen carrier can be expected to be negligible in fixed-bed systems, and cyclones and filters for gas-solid separation are not required. Moreover, a better utilization of the oxygen carrier is achieved because fixed beds increase the degree of conversion between the reduced and the oxidized forms of the carrier particles. There is also an extensive bank of experience in the industry with pressure and temperature swing adsorption systems that could be adapted to CLC fixed-beds configurations. Early works on "unmixed reforming" concepts [29], provided experimental evidence that the redox reactions involved in CLC processes evolve very quickly in narrow reaction fronts along dynamically operated fixed-bed reactors. More recent studies have been focused on demonstrating theoretically and experimentally the feasibility of the CLC concept in fixed-bed configurations for CO2 capture on a large scale [30-38].

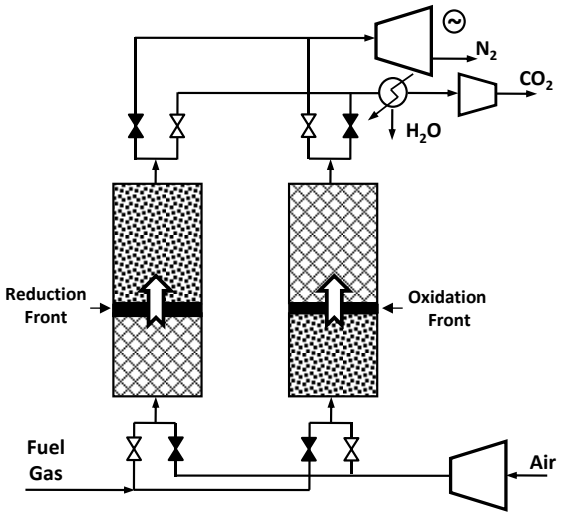

Fig. (1). Basic scheme of a CLC system with alternating fixed-bed reactors for power generation.

The main drawback of fixed-bed systems is the need for heat management strategies to control the change in temperature as the reaction fronts advance through the reactors, especially during the exothermic metal oxidation stage. Since most of the oxygen carriers proposed in the literature lose their reactivity and tend to agglomerate at temperatures higher than 1100-1200 ºC [8-10], a careful control of the temperature in the reaction fronts is essential, when highly exothermic oxidation reactions are taking place. Mass and heat balances show that the change in temperature in the reaction fronts is determined by the composition, thermal properties and temperature of the inlet gas, as well as by the initial temperature, thermal properties and inert content of the solids bed [27, 32]. During the CLC operation, the reaction and solid/gas heat exchange fronts move along the fixed beds at different velocities, depending mainly on the concentration and molecular weights of the reactants and on the stoichiometry of the reactions. A similar phenomenon is observed in the catalytic oxidation of fuel gas when the process is performed at different operating temperatures [39]. Two main heat strategies are proposed in the literature to control the maximum temperature in the reaction fronts. One option is to perform the oxidation stage by feeding into the air reactor a stream of air at high pressure and at moderate temperature [27, 30]. Under these conditions, the reaction front moves forward faster than the solid/gas heat exchange front. This means that the gas arrives at the reaction front already preheated by the previously oxidized solids, which in turn have been heated by the heat released in the oxidation reaction. When oxygen carriers with a high carrying capacity and a high oxidation enthalpy, such as Ni or Cu, are used, only low metal loadings (lower than 20 wt.%) are needed

in order to limit the increase in temperature during the operation. Using a large amount of inert material makes it possible to separate the advance of the reaction and heat exchange fronts, so that there will be a larger mass of solids between them able to absorb the heat released from the oxidation reaction. One of the problems with this option is the need to use large high-pressure reactors to accommodate a large fraction of inert solids for a given flow of fuel gas fed into the system. Another strategy for the heat management of a chemical looping system is to control the increase in temperature during the oxidation stage by recycling a large amount of the cooled N_2 product gas in order to dilute the O_2 fed into the air reactor [32]. The reaction front will then advance at a slower velocity than the heat exchange front and it will be possible to operate with very high active contents of the oxygen carrier without exceeding the maximum temperature allowable in the reaction front. This alternative allows a more compact reactor design at the expense of an increase in the consumption of energy and equipment cost associated with the recirculation of part of the product gas back to the air reactor inlet.

The second strategy has already been implemented in a previous work [40] to control the temperature in a Ni-based CLC system using methane as fuel. A preliminary conceptual design showed that a sequence of five stages was necessary to carry out the reactions involved and to solve the heat management problems typical of a fixed-bed system. The main objective of that study was to minimize the total volume of reactors required. It was calculated that eight reactors operating in synchronized mode were needed to ensure a continuous flow of product gas at a sufficiently high temperature and pressure for its expansion in a gas turbine for power generation. Such a large number of reactors necessitated a relatively complex switching-valve system to function adequately and able to withstand gases at high temperature.

The objective of the present study is to design a more compact Ni-based CLC process system in fixed beds with the smallest possible number of reactors for carrying out the complete process (at the expense of a slightly larger reactor volume). This will allow a simpler overall system to carry out the synchronized operation. Moreover, an approach about the thermal integration of the CLC system for power generation has been carried out to confirm the potential of this process for a future development as power generation system with CO_2 capture.

2. PROCESS DESCRIPTION, REACTOR DESIGN AND PROCESS INTEGRATION

A basic reactor model has been used to approximately represent the performance of the fixed-bed reactors in each stage of the process. The reactions involved are assumed to be fast enough to take place in very narrow reactions fronts that move forward as the reacting gases are fed in and the solids are converted. An ideal plug flow model is considered to be a reasonable representation of the flow pattern, in which the solid-gas reactions proceed rapidly and axial gas dispersion effects can be neglected. These assumptions, common in other fixed-bed catalytic reactions [41], were initially adopted by Noorman et al. [27] to theoretically describe the cyclic operation of fixed-bed reactor systems for chemical looping combustion applications. They have also been applied to design a reaction system involving sorption enhanced reforming [32]. These assumptions have been experimentally demonstrated in recent CLC works [38, 42, 43]. Under these conditions, the velocity of the reaction fronts along the fixed beds (ur) can be calculated by means of a mass balance in the reaction front as follows [27]:

$$u_r = \frac{\rho_g u_g x_g M_s}{\varepsilon \rho_s x_s M_g \varphi} \quad (1)$$

where ϱg and ϱs represent the density of the gas and the solid, respectively, ug is the superficial gas velocity, xiis the mass fraction of the gas/solid component, Mi is the molecular weight, ε is the porosity, and φ is the stoichiometric factor of the gas/solid reaction.

Furthermore, when the reactions involved are not thermally neutral and/or when the temperatures of the gases and the solids in contact are different, heat exchange fronts are also formed. As a result of the convective gas flow, the heat fronts also move towards the reactor exit at velocities (ue) that can be estimated by means of heat balances in the heat exchange fronts as follows [27]:

$$u_e = \frac{\rho_g u_g c_{p,g}}{\epsilon \rho_s c_{p,s}} \quad (2)$$

The maximum increase in temperature (ΔTmax) achieved during a gas/solid exothermic reaction can be calculated by an energy balance at the reaction front, assuming that the heat released when the gas reacts is absorbed by the solids. This mainly depends on the enthalpy and the stoichiometry of the reaction and the concentration of the gas/solid reagents, and can be estimated as follows [27]:

$$\Delta T_{max} = \frac{-\Delta H_r}{\frac{c_{ps} M_s}{x_s \varphi} - \frac{c_{pg} M_g}{x_g}} \quad (3)$$

Fig. (**2**) shows the flow diagram of the proposed CLC system. The proposed process comprises at least four fixed-bed reactors operating in parallel and common elements of conventional natural gas combined cycles (NGCC), i. e., an air compressor, a gas turbine, a heat recovery steam generator (HRSG) and a compressor for the recirculation of the N_2 discharged downstream of the HRSG. A heat exchanger and a compressor are required to cool down, purify and compress the CO_2-rich stream finally obtained, as happens in any CCS system. Additional elements are also needed, such as blower/fan to recompress the recycled stream of CO_2 with steam in the reduction stage, heat exchangers and an expander to condition the temperature and efficiently recover the excess of heat of certain gas streams (see Fig. 2). The performance of the reduction and oxidation stages during the cyclic operation of the process is described in Fig. 3. Assuming an intense heat transfer between the gases and solids, the temperature of the gases and solids can be considered very similar at any point

along the reactors. This makes it possible to explain each stage using a single axial temperature profile along the entire reactor [27, 32, 44]. A reference case with an inlet flow of 10 kg/s of methane (equivalent to around 500 MWth) and using a Ni/Al2O3 oxygen carrier (60% wt. Ni) has been adopted by way of example to show the feasibility of this CLC system at a large scale. A maximum temperature of 1200 ºC is targeted for the design of the oxidation stages in order to ensure that the high stability and reactivity of the Ni-based carrier are maintained after multiple reduction and oxidation cycles. An operating pressure of 22 bar has been selected in order to achieve the highest energy efficiency in the downstream gas turbine [17] and assuming reasonable pressure drops along the fixed beds. Table **1** summarizes the input operating conditions chosen for the case study, which have been chosen according to the literature about CLC in fixed-bed reactors [33-36]. Table **2** indicates the flow rate, composition, temperature and pressure of the gas streams showed in Figure 2, which were obtained by solving the mass and heat balances related to each stage of the process.

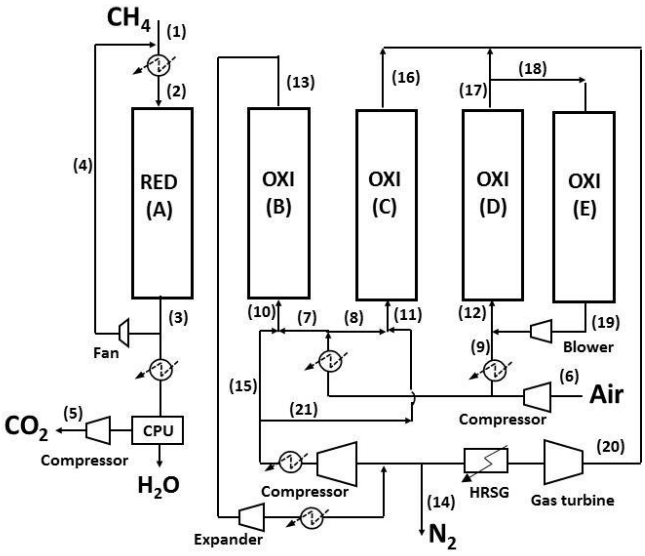

Fig. (2). Process flow diagram of the proposed CLC system using fixed-bed reactors arranged in parallel.

Table 1. Operating conditions and reactor characteristics for the reference case study [33-36].

Parameters	Values
Inlet CH_4 mass flow, kg/s	10
Pressure, bar	22
Temperature (maximum), ºC	1200
Ni content in solid, wt.%	60
Particle size, m	0.01
Bed porosity	0.5
Bed density, kg/m^3	1700

At the beginning of the reduction stage (A), the Ni-based carrier is completely oxidized, as a result of a previous oxidation stage (D) (described below). Part of the packed bed was left at 1200 ºC (Ts1 in Fig. **3**), while the rest of the solids are at 150 ºC (Ts2 in Fig. **3**). A stream of 0.625 mol/s of pure methane (stream 1 in Fig. **2**) is fed in at 22 bar by the part of the bed that is at 1200ºC, which is at a sufficiently high temperature to cause the rapid and complete oxidation of CH4 to CO_2 and H_2O by the NiO contained in the bed, which is reduced to Ni [26, 45]. As the bed is initially divided into two parts at different temperatures, two heat exchange fronts (e1 and e2 in Fig. **3**) advancing to the reactor exit during the operation are formed. Since the reduction of NiO with methane is highly endothermic (ΔHr=134 kJ/mol), a drop in temperature (ΔTred in Fig. **3**) is produced in the reduction front (r in Fig. **3**). Therefore, a significant part of the solids bed must initially be at 1200 ºC in order to maintain the advance of the reaction front to the end of the stage. Under the conditions established for the reduction stage, the reduction front (r) moves forward faster than the heat exchange fronts (e1 and e2), and consequently, a heat plateau (at T1) behind the reduction front is formed. In this situation, the gas arrives at the reaction front already preheated by the reduced solids, which in turn are cooled down from 1200ºC to T1. The recirculation of part of the product gas (stream 4 in Fig. **2**) back to the reactor inlet increases the inlet gas flow to the reduction stage (stream 2 in Fig. **2**), which accelerates the advance of the heat exchange fronts. This allows the reduction stage (A) to begin with only a part of the bed at 1200 ºC. Consequently, a higher proportion of the heat generated during the subsequent Ni oxidation stages can be used to produce N_2 at a high enough temperature and pressure to be expanded in a gas turbine for power generation. However, the shorter distance between the advance of both fronts (r) and (e2) causes a further drop in temperature in the reduction front, because there is now a smaller mass of solids at 1200ºC for supplying the heat required to carry out the endothermic reduction of NiO with methane [40].

The recirculation of around 54 vol.% of the product gas (stream 3 in Fig. **2**) to the reactor inlet allows the reaction front (r) to advance only 1.3 times faster than e2, estimated by Eq. (1) and Eq. (2), and therefore, the reduction stage can be carried out by starting out with only 38 wt.% of the bed at 1200 ºC. Under these conditions, the decrease in temperature in the reduction front, calculated by Eq. (3), amounts to 700 ºC, and therefore the reduced solids are left behind the reaction front at 500 ºC (T1 in Fig. **3**). This temperature is sufficiently high to initiate a rapid oxidation of the Ni-based carrier in the following reaction stage [8]. For the reference case, a total flow rate of 2.79 kmol/s (stream 2 in Fig. **2**) is fed into the reduction stage (A), which is previously preheated up to 450 ºC. This particular choice of operating conditions is intended to allow the reaction front (r) to catch up with the heat exchange front (e2) at the reactor exit, and therefore, as the product gas is released, it will be at the initial temperature of the solids closest to the reactor exit (150 ºC). Once the bed has been completely reduced (t=tend in Fig. 3), the solids that have been traversed by all the fronts are left at the temperature of the inlet gas (450 ºC), which is around 75 wt.% for this reference case. The rest of the bed (around 25 wt.%) will

remain at 500 ºC (T1 in Fig. **3**). The product gas that is not recirculated is guided to the CO_2 purification unit (CPU), giving rise to a flowrate of 0.612 kmol/s of pure CO_2 (about 2% of the incoming CO_2 is unavoidably vented to atmosphere [46]), which is obtained ready for compression and subsequent storage or reuse in chemical applications [47].

Once the oxygen carrier has been completely reduced, the subsequent oxidation stage is initiated by feeding in air at 22 bar through the part of the reactor where the solids are at the highest temperature (500 ºC in the reference case). The strategy adopted to moderate the increase in temperature in the oxidation front is to recirculate part of the gas discharged during the oxidation, which is mainly composed of N_2, and to dilute the O_2 in the feed. Under these circumstances, the reaction front (r in Fig. 3) will move forward more slowly than the heat exchange front (e1) and the solids located between both fronts will absorb the heat released in the oxidation front.

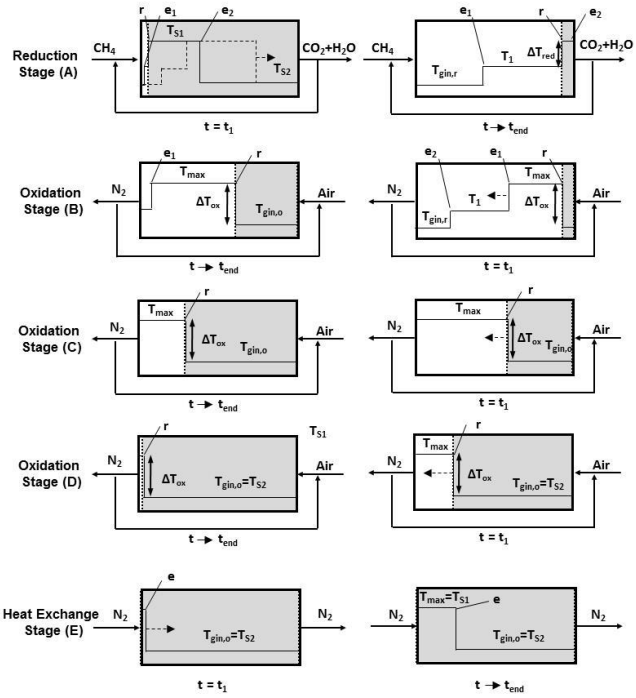

Fig. (3). Evolution of the T profile during the stages of the CLC process (r: reaction front, ei: heat exchange front, white zone: reduced oxygen carrier, grey zone: oxidized oxygen carrier).

As can be seen in Fig. 3, the gas arrives at the reaction front at the inlet gas temperature (Tgin,o) and heats up due to the exothermicity of the oxidation reaction (ΔHr=-478 kJ/mol O_2). The heat released is transported forward by the nitrogen that leaves the reaction front and, as a result, the solids downstream (initially at T1) will undergo an increase in temperature up to Tmax. Meanwhile, the solids that have already been oxidized are left behind at the temperature of the inlet gas (Tgin,o). Under these conditions, the inlet gas temperature needs to be preferably low in order to moderate the maximum temperature achieved in the oxidation front. The compressed air at 22 bar comes from the compressor at around 450 ºC [35] and it is subsequently cooled down to 150 ºC. Heat exchangers (see Fig. **2**) are then required to remove the excess of heat before the compressed air is mixed with the recycled nitrogen and fed into stage (B) and stage (C). This excess of heat will be used for preheating the feed of the reduction stage (A). Since the Ni-based carrier contains 60 wt.% of active phase, it is necessary to dilute the O_2 in the feed down to 5.3 vol.% in order to limit the increase of temperature in the oxidation front (ΔTox in Fig. **3**) up to 1050ºC, and therefore, to keep the maximum temperature during the oxidation within the targeted limit of 1200 ºC (Eq. 3). This means that approximately 80 vol.% of the exhaust nitrogen must be recirculated to the reactor inlet during the oxidation stage. As the bed is initially divided into two zones with different temperatures (T1 and Tgin,r, 500ºC and 450ºC, respectively in the reference case) and the feed is introduced at another temperature (150 ºC), two heat exchange fronts, e1 and e2 are formed. They move forward throughout the oxidation stage at the velocities estimated by Eq. (1) and Eq. (2). For the conditions chosen for the reference case, a flow of 6.69 kmol/s (stream 10 in Fig. 2) of diluted air is fed into stage (B) and the heat exchange front (e1) will advance approximately 3.5 times faster than the reaction front (r). The oxidation stage (B) takes place while the heat exchange front (e1) has not yet arrived at the reactor exit and it finishes when the flue gas is about to be released at the maximum temperature (Tmax). During the part of the stage (B) in which the heat exchange front (e2) has still not reached the reactor exit (approximately 75% of the duration of the stage B), the product gas is discharged at 450 ºC (Tgin,r in Fig. **3**), which is the temperature of the solids located closest to the exit. During the rest of the stage, the product gas is released at 500 ºC (T1 in Fig. **3**). At the end of stage (B), around 30% of the bed has been oxidized and is left at 150 ºC. The rest of the bed will remain as NiO (over alumina) and at 1200ºC (Tmax in Fig. **3**). As explained above, these results are the result of solving the mass and energy balances in every stage of the process.

The oxidation will continue during stage (C), when the flue gas is discharged at 1200 ºC, and is subsequently fed into a gas turbine for the generation of power. This temperature is lower than the nominal inlet temperature of modern gas turbines (1400-1450ºC) [17]. One option to increase the efficiency of CLC system would be to burn an additional flow of methane in a combustor placed upstream the gas turbine in order to increase the temperature of the gas fed into the gas turbine close to the optimum value, at the expense of higher CO_2 emissions in the process [18], but this alternative is out of the scope of this work. At the conditions chosen for this case study, the total molar flow introduced into the reactor during stage (C) is about 13.4 kmol/s (stream 11 in Fig. **2**), whilst the nitrogen obtained at the outlet is around 12.7 kmol/s (stream 16 in Fig. **2**). A large fraction of the cooled N_2 exhaust gas from the combined cycle will be recirculated and recompressed back in through the reactor inlet in order to dilute the incoming air and therefore control the maximum temperature during the operation. This arrangement is similar to that of flue gas recirculation systems (FGR) in large-scale NGCC designed to increase the concentration of CO_2 in flue gases before they enter the postcombustion capture systems [48].

Table 2. Temperature, flow rate and composition of the gas streams of the CLC process for the reference case (*around 75% of the duration of stage (B) stream 13 is emitted at 450ºC, while the remaining 25% is released at 500ºC) (from equations 1-3) [27].

Stream	T, ºC	P, bar	M, kmol/s	Molar composition, %				
				CH_4	H_2O	CO_2	O_2	N_2
1	25	22.0	0.625	100	-	-	-	-
2	450	22.0	2.790	22.4	51.7	25.9	-	-
3	150	21.8	4.040	-	66.7	33.3	-	-
4	150	22.0	2.165	-	66.7	33.3	-	-
5	30	110	0.612	-	-	100	-	-
6	25	1.0	5.952	-	-	-	21.0	79.0
7	150	22.0	1.695	-	-	-	21.0	79.0
8	150	22.0	3.393	-	-	-	21.0	79.0
9	805	22.0	0.865	-	-	-	21.0	79.0
10	150	22.0	6.693	-	-	-	5.3	94.7
11	150	22.0	13.399	-	-	-	5.3	94.7
12	1100	22.0	3.415	-	-	-	5.3	94.7
13	450/500*	19.8	6.337	-	-	-	-	100
14	30	1.0	4.702	-	-	-	-	100
15	150	22.0	4.998	-	-	-	-	100
16	1200	19.9	12.687	-	-	-	-	100
17	1200	21.3	3.233	-	-	-	-	100
18	1200	21.3	2.550	-	-	-	-	100
19	150	20.8	2.550	-	-	-	-	100
20	1200	19.9	13.370	-	-	-	-	100
21	150	22.0	10.006	-	-	-	-	100

During the following stage (D), the oxidation of the bed with N_2 recycle will continue until all the Ni-based particles are completely oxidized. As explained above, as the oxidation front moves forward, the converted solids are left behind at the inlet gas temperature, which is normally too low for another reduction of NiO to Ni (150 ºC in this reference case). Therefore, an additional heat exchange stage (E) is needed in the CLC process, in which a fraction of the product gas discharged at the maximum temperature of 1200 ºC during stage (D) will be used to raise the temperature of part of the reactor (E), which had been left oxidized but at a low temperature (i.e. 150 ºC). As mentioned above, for the reference case only 38 wt.% of the bed initially at 1200 ºC is required to accomplish the reduction stage. An overall heat balance defines the transition point between stage (C) and stage (D) once the heat requirements for carrying out a new reduction stage (A) are known. Under these conditions, stage (D) begins when nearly 85 wt% of the solids bed has been oxidized. During stage (D), a flow of around 3.4 kmol/s (stream 12 in Fig. **2**) will be introduced at 1200ºC. Meanwhile, about 2.5 kmol/s will be led to stage (E) for preheating purposes. The rest of the N_2 produced during the oxidation, that accounts for 13.37 kmol/s (stream 20), will be guided to the combined cycle for power generation.

The number of reactors required for the complete CLC process (following the sequence of five stages explained above) must be kept to a minimum in order to minimize the equipment cost. However, a larger number of reactors may be needed, since the gas flow rates calculated for every stage must be accommodated at reasonable gas velocities in order to avoid excessive pressure drops. Taking into account the operating conditions listed in Table **1** and the inlet flow rates calculated for each stage (see Table **2**), it seems that every stage can be carried out in one reactor, excepting stage (C) with much higher inlet flowrate, thereby requiring there two reactors performing simultaneously. Therefore, a total of six reactors operating in synchronized mode will be required, i. e., one reactor for stage (A), one reactor for stage (B), two reactors for stage (C), one reactor for stage (D) and one reactor for stage (E). A very short rinse step is needed between the reduction and oxidation stages in order to avoid unwanted reactions during the transition periods. However, the duration of the rinse steps can be considered negligible in relation to the total duration of the cycle because only five reactor volumes of inert gas would be required for a complete rinse (i.e. rinse durations of less than one minute) [46]. The operational diagram of the proposed CLC system is represented in Fig. **4** for a specific point in time. It is similar to other fixed-bed configurations used for H2 production [46, 49-51] and other CLC applications [28, 35]. Fig. **5** shows the evolution of composition and temperature of the outlet gas in every stage of the proposed CLC process. In contrast to other CLC configurations carried out in fixed beds [28, 35, 44], the CO_2-rich gas produced during the reduction stage is emitted at very low temperature (150 ºC), and therefore, no heat can be recovered from it for power generation. However, the nitrogen generated during the oxidation stages is released mostly at the highest temperature, which should lead to a potentially higher plant efficiency [35], since a higher fraction of the heat generated during the exothermic oxidation of Ni to NiO would be aimed at the generation of power in the gas turbine.

The geometry of each reactor and the duration of a single stage are defined as follows. The cross-sectional area and the minimum time required to accomplish each single stage must be able to accommodate the flows of the inlet gases at reasonable gas velocities and pressure drops. Larger reactors operating at high pressure require more costly equipment, thicker walls and additional security arrangements. To choose a specific value for these design variables, the effect of the duration of the cycles on reactor geometry and pressure drop was studied assuming a maximum inlet flow per stage of 6.69 kmol/s (that corresponds to the feed into stage B), a pellet size of 0.01 m, a void fraction of 50% and a bed densitity of 1700 kg/m3 when the Ni-based carrier is completely oxidized (see Table **1**).

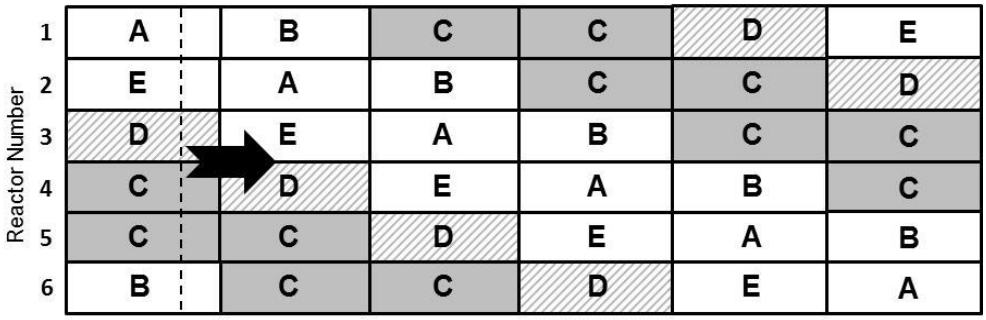

Fig. (4). Operational diagram of the proposed CLC system (the dotted line represents a snapshot of the process for a specific point in time; stages in grey produce gas at Tmax for power generation).

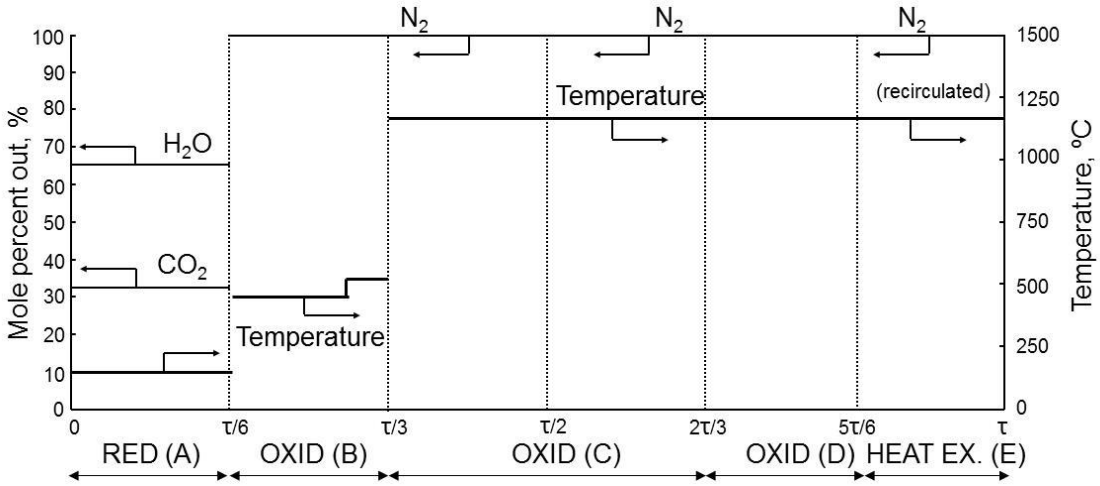

Fig. (5). Evolution of composition and temperature of the outlet gas in every stage of the proposed CLC process.

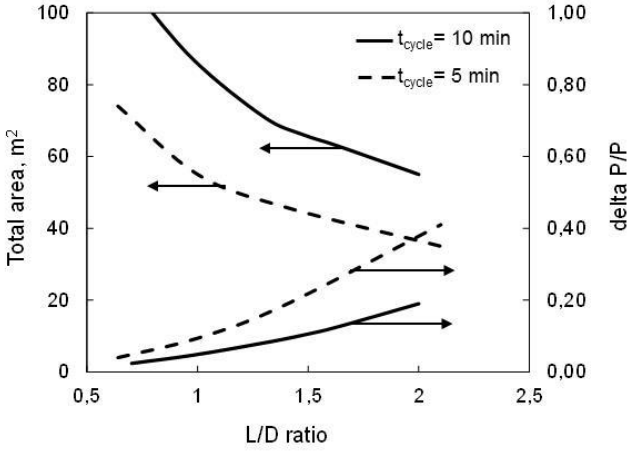

Fig. (6). Effect of cycle duration on reactor geometry and pressure drop.

As can be seen in Fig. 6, shorter cycle durations allow smaller cross-sectional areas to convert the same amount of gas fed into the system. Larger reactor lengths combined with smaller diameters (i. e. higher L/D ratios) also reduce the total area required. However, these conditions will cause higher pressure drops, resulting in an increase in the energy needed to recompress the gas streams involved in the process. For the operating conditions and reactor characteristics assumed in the reference case, a minimum duration of about 10 minutes can be considered as a reasonable time to complete each single stage of the CLC process. Assuming a L/D ratio of about 1.7 and a maximum pressure drop of about 10% in each stage, the full process scheme for 10 kg/s of methane fed into the reduction stage will require 6 reactors, 7 m long with an inner diameter of 4 m (that means a total cross-sectional area of around 75.4 m2).

The integration of the proposed fixed-bed Ni-based CLC system in a natural gas combined cycle (NGCC) has also been carried out to evaluate the competitiveness of this technology with respect to benchmarks for power generation with an without CO_2 capture. The technology that represents the state-of-the-art of power plants using methane as fuel is the NGCC because of its relatively high efficiency and moderate capital cost [51]. The power generation process with CO_2 capture taken as reference in this work consists of an Auto Thermal Reformer (ATR), followed by two-stage water gas shift (WGS) section, a methyldiethanolamine (MDEA) chemical absorption process to remove the CO_2 from the product gas and a final combined cycle power plant. A detailed description including a comprehensive thermodynamic assessment of these power generation processes with and without CO_2 capture can be found elsewhere [51- 55]. Table 3 summarizes the main sources of energy production and consumption of the benchmark plants together with those obtained for the proposed fixed-bed CLC system.

Table 3. Performance obtained for the Ni-based fixed-bed CLC and for the benchmark NGCC with and without CO_2 capture.

	Benchmark plants		
	NGCC w/o capture [51-53]	**ATR+MDEA NGCC[51-53]**	**Fixed-bed CLC NGCC**
Gas turbine (GT), MW	197	287.7	283.1
GT Auxiliaries, MW	-0.7	-1.0	-1.0
Steam turbine, MW	113.3	157.2	99.1
Steam cycle pumps, MW	-1.4	-3.2	-1.5
N_2 expander, MW	-	-	68.27
Air compressor, MW	-	-7.1	-80.27
N_2 compressor, MW	-	-	-73.5
Plant auxiliaries, MW	-	-3.6	-3
Fans/Blowers, MW	-	-	-4.5
CO_2 compressor, MW	-	-15.2	-10.6
Net power, MW	308.2	414.9	276.1
Thermal input (LHV), MW	524	813.4	500
Net efficiency, %	58.8	51.0	55.2
CO_2 capture efficiency,%	-	91.6	98.0

The CO_2 capture efficiency is calculated as the ratio between the molar flow rate of CO_2 obtained downstream of the CO_2 compression and purification unit (CPU) and the molar flow rate of CO_2 associated with the total CH4 fed into the plant. The commercial NGCC shows a net efficiency of about 59%, in which around 66% of the energy generated comes from the gas turbine (GT) and the rest from the steam turbine (ST). For the ATR plant with MDEA absorption, an energy efficiency of around 51% is achieved. This 8 points of energy penalty are associated with the CO_2 capture process (almost 4% of the energy produced in this plant is consumed during the CO_2 compression step). When compared with the ATR+MDEA plant, a significantly higher net efficiency is achieved in the fixed-bed CLC process (55.2% vs 51%), including greater CO_2 capture ratio (98% vs 91.6%), as can be seen in Table **3**. In the proposed CLC system, a larger proportion of the heat generated during the Ni oxidation stages can be used for power generation by expanding the high temperature pressurized N_2 in a gas turbine. About 382 MW are obtained in the combined cycle from the 500 MW of input energy. The main energy consumption comes from the air compressor (needed for the oxidation stages) and from the N_2 compressor (used to supply again in the system the cooled N_2 exhaust gas from the combined cycle), accounting for 80 MW and 68 MW, respectively. Energy consumed in the compression units has been calculated assuming a polytrophic efficiency of 80% and a mechanical-electric efficiency of 94%. Other elements, such as, water pumps or condensers upstream of the PSA and CPU are assumed to have the same energy demand to analogous devices in the benchmark plants for the sake of simplicity. As can be seen, nearly 4 points higher than that obtained in the benchmark plant with CO_2 capture can be achieved in the Ni-based fixed-bed CLC system, which demonstrates the potential of this novel process as a future power generation system with near zero CO_2 emissions, although a more detailed process integration together with a cost analysis of the plant (out of the scope of this work) is needed to confirm its feasibility.

CONCLUSIONS

Fixed-bed configurations using Ni-based materials have been shown to be a valid alternative for carrying out the chemical looping combustion of methane at high pressure as a means of overcoming the characteristic problems related to high-pressure fluidized bed concepts, including trace emissions of hazardous metals. However, more complex heat management strategies and the need for switching-valves able to cope with gases at very high temperatures are required in packed-bed systems. Gas recycles allow the advance of the reaction and heat exchange fronts to be controlled, enhancing the heat management during the CLC operation. Basic reactor models used to calculate the variation of temperature in the reaction fronts of CLC in fixed beds show that the increase in temperature in the oxidation front can be kept within reasonable bounds by introducing cooled recycles of nitrogen into the oxidation stages. These conditions permit the use of oxygen carriers with a very high Ni content (≥60 wt.%) allowing more compact reactor designs. Moreover, the recirculation of part of the CO_2 and H_2O produced in the reduction of NiO to Ni with methane make it possible for the reaction and heat exchange fronts to advance closer during the operation, which means that the reduction stage can be initiated with a lower fraction of solids at high temperature. As a result, a higher proportion of the heat generated during the oxidation stages can be used for power generation by expanding the high temperature pressurized N_2 in a gas turbine. A sequence of five stages is necessary to carry out the reactions involved and satisfy the energy requirements of the process. A configuration design assuming 10 kg/s of methane has led to the conclusion that a minimum of six reactors performing in synchronized mode will be required to accomplish the complete process. For the operating conditions and reactor characteristics of this study, a minimum duration of about 10 minutes can be considered as a reasonable time for each single stage of the CLC process. To define the size of the reactors, a L/D ratio of about 1.7 and a maximum pressure

drop of about 10 % has been assumed. It has been shown that a full process scheme would require four reactors, 7 m long with an inner diameter of 4 m. About 55% of energy efficiency with 98% of CO_2 capture efficiency have been calculated, which means only 3.5 points of energy penalty compared to a conventional NGCC without CO_2 capture. These results confirm the potential of this novel systems as a future power generation process with near zero CO_2 emissions and reduced energy penalty.

NOMENCLATURE

cpi	specific heat capacity of component i, kJ/mol ºC
ΔHr	enthalpy of the reaction, kJ/mol
Mi	molecular weight of component i, kg/mol
P	pressure, bar
t	time, s
Tg,in	inlet gas temperature, ºC
Tmax	maximum temperature, ºC
Ts0	initial temperature of bed reactor, ºC
ΔTmax	maximum adiabatic temperature increase, ºC
ue	heat exchange front velocity, m/s
ug	gas velocity, m/s
ur	reaction front velocity, m/s
xi	weight fraction of component i, dimensionless

GREEK LETTERS

ρi	density of component i, kg/m3
ε	porosity, dimensionless
φ	stoichiometric factor, dimensionless

CONFLICT OF INTEREST

The author declares no conflicts of interest

REFERENCES

[1]. Edenhofer O, Pichs-Madruga R, Sokona Y, Farahani E, Kadner S, Seyboth K, Adler A, Baum I, Brunner S, Eickemeier P, Kriemann B, Savolaninen J. Climate Change 2014: Mitigation of Climate Change. Contribution of Working Group III to the Fifth Assessment Report of the Intergovernmental Panel on Climate Change. Cambridge University Press, Cambridge, United Kingdom and New York, NY, USA, 2014.

[2]. IEA, Energy Technology Perspectives - Catalysing Energy Technology Transformations. 2017, International Energy Agency: Paris, France.

[3]. Olivier JGJ, Schure KM, Peters JAHW. Trends in global CO_2 and total greenhouse gas emissions. PBL Netherlands Environmental Assessment Agency, 2017.

[4]. Boot-Handford ME, Abanades JC, Anthony EJ, Blunt MJ, Brandani S, Mac Dowell N, Fernandez JR, Ferrari MC, Gross R, Hallett JP, Haszeldine RS, Heptonstall P, Lyngfelt A, Makuch Z, Mangano E, Porter RTJ, Pourkashanian M, Rochelle GT, Shah N, Yao JG, Fennell PS. Carbon capture and storage update. Energ Environ Sci 2014; 7, 130-89.

[5]. Abanades JC, Arias B, Lyngfelt A, Mattisson T, Wiley DE, Li H, Ho MT, Mangano E, Brandani S. Emerging CO_2 capture systems. Int J Greenh Gas Con 2015; 40, 126-66

[6]. Lyngfelt A, Leckner B, Mattisson T. A fluidized-bed combustion process with inherent CO_2 separation; application of chemical-looping combustion. Chem Eng Sci 2001; 56, 3101-13.

[7]. Ishida M, Yamamoto M, Ohba T. Experimental results of chemical-looping combustion with NiO/NiAl2O4 particle circulation at 1200 degrees C. Energy Convers Mgmt 2002; 43, 1469-78.

[8]. Adanez J, Abad A, Garcia-Labiano F, Gayan P, de Diego LF. Progress in Chemical-Looping Combustion and Reforming technologies. Prog Energ Combust 2012; 38, 215-82.

[9]. Fan LS, Zeng L, Wang W, Luo S. Chemical looping processes for CO_2 capture and carbonaceous fuel conversion - prospect and opportunity. Energ Environ Sci 2012; 5(6), 7254-80.

[10]. Adánez J, Abad A, Mendiara T, Gayán P, de Diego LF, García-Labiano F. Chemical looping combustion of solid fuels. Progress Energ Comb Sci 2018; 65, 6-66.

[11]. Johansson E, Mattisson T, Lyngfelt A. A 300 W laboratory reactor system for chemical-looping combustion with particle circulation. Fuel 2006; 85, 1428-38.

[12]. de Diego LF, García-Labiano F, Gayán P, Celaya J, Palacios JM, Adánez J. Operation of a 10 kWth chemical-looping combustor during 200 h with a CuO-Al2O3 oxygen carrier. Fuel 2007; 86, 1036-45.

[13]. Linderholm C, Abad A, Mattisson T, Lyngfelt A. 160h of chemical-looping combustion in a10kW reactor system with a NiO-based oxygen carrier. Int J Greenh Gas Con 2008; 2, 520-30.

[14]. Kolbitsch P, Bolhàr-Nordenkampf J, Pröll T, Hofbauer H. Operating experience with chemical looping combustion in a 120kW dual circulating fluidized bed (DCFB) unit. Int J Greenh Gas Con 2010; 4, 180-5.

[15]. Kronberger B, Lyngfelt A, Löffler G, Hofbauer H. Design and fluid dynamic analysis of a bench-scale combustion system with CO_2 separation-chemical looping combustion. Ind Eng Chem Res 2005; 44, 546-56.

[16]. Abad A, Mattisson T, Lyngfelt A, Rydén M. Chemical-looping combustion in a 300 W continuously operating reactor system using a manganese-based oxygen carrier. Fuel, 2006; 85, 1174-85.

[17]. Brandvoll Ø, Bolland O. Inherent CO_2 capture using chemical looping combustion in a natural gas fired power cycle. J Eng Gas Turb Power 2004; 126, 316-21.

[18]. Consonni S, Lozza G, Pelliccia G, Rossini S, Saviano F. Chemical-looping combustion for combined cycles with CO_2 capture. J Eng Gas Turb Power 2006; 128, 525-34.

[19]. Kvamsdal HM, Jordal K, Bolland O. A quantitative comparison of gas turbine cycles with CO_2 capture. Energy 2007; 32(1), 10-24.

[20]. Naqvi R, Bolland O. Multi-stage chemical looping combustion (CLC) for combined cycles with CO_2 capture. Int J Greenh Gas Con 2007; 1, 19-30.

[21]. Xiao R, Song Q, Song M, Lu Z, Zhang S, Shen L. Pressurized chemical-looping combustion of coal with an iron ore-based oxygen carrier. Combust Flame 2010; 157, 1140-53.

[22]. [22] Bischi A, Langorgen O, Saanum I, Bakken J, Seljeskog M, Bysveen M, Morin X, Bolland O. Design study of a 150 kWth double loop circulating fluidized bed reactor system for chemical looping combustion with focus on industrial applicability and pressurization, Int J Greenh Gas Con 2011; 5, 467-74.

[23]. Brandvoll O, Kolbeinsen L, Olsen N, Bolland O. Chemical Looping Combustion – Reduction of nickel oxide/nickel aluminate with hydrogen. Chem Eng Trans 2003; 3, 105-10.

[24]. Mattisson T, Johansson M, Lyngfelt A. The use of NiO as an oxygen carrier in chemical looping combustion. Fuel 2006; 85, 736–47.

[25]. Zafar Q, Mattisson T, Gevert B. Integrated Hydrogen and Power Production with CO_2 Capture Using Chemical-Looping Reforming-Redox Reactivity of Particles of CuO, Mn2O3, NiO, and Fe2O3 Using SiO2 as a Support. Ind Eng Chem Res 2005; 44, 3485-96.

[26]. Abad A, Adánez J, García-Labiano F, de Diego LF, Gayán P, Celaya J. Mapping of the range of operational conditions for Cu-, Fe-, and Ni-based oxygen carriers in chemical-looping combustion. Chem Eng Sci 2007; 62(1), 533-49.

[27]. Noorman S, van Sint Annaland M, Kuipers H. Packed bed reactor technology for chemical-looping combustion, Ind Eng Chem Res 2007; 46, 4212-20.

[28]. Hamers HP, Romano MC, Spallina V, Chiesa P, Gallucci F, Van Sint Annaland M. Comparison on process efficiency for CLC of syngas operated in packed bed and fluidized bed reactors. Int J Greenh Gas Con 2014; 28, 65-78.

[29]. Kumar RV, Lyon RK, Cole JA. Unmixed reforming: a novel authotermal cycling steam reforming process. In Advances in Hydrogen Energy, Higham, MA, USA; 2000.

[30]. Noorman S, Gallucci F, van Sint Annaland M, Kuipers H. A theoretical investigation of CLC in packed beds. Part 2: Reactor model. Chem Eng J 2011; 167, 369-76.

[31]. Noorman S, Gallucci F, van Sint Annaland M, Kuipers H. Experimental investigation of chemical-looping combustion in packed beds: a parametric study. Ind Eng Chem Res 2011; 50, 1968-80.

[32]. Fernández JR, Abanades JC, Murillo R, Grasa G. Conceptual design of a hydrogen production process from natural gas with CO_2 capture using a Ca-Cu chemical loop. Int J Greenh Gas Con 2012; 6, 126-41.

[33]. Spallina V, Gallucci F, Romano MC, Chiesa P, Lozza G, van Sint Annaland M. Investigation of heat management for CLC of syngas in packed bed reactors. Chem Eng J 2013; 225, 174-91.

[34]. Hamers HP, Gallucci F, Cobden PD, Kimball E, Van Sint Annaland M. A novel reactor configuration for packed bed chemical-looping combustion of syngas. Int J Greenh Gas Con 2013; 16, 1-12.

[35]. Spallina V, Romano MC, Chiesa P, Gallucci F, Van Sint Annaland M, Lozza G. Integration of coal gasification and packed bed CLC for high efficiency and near-zero emission power generation. Int J Greenh Gas Con 2014; 27, 28-41.

[36]. Spallina V, Chiesa P, Martelli E, Gallucci F, Romano MC, Lozza G, van Sint Annaland M. Reactor design and operation strategies for a large-scale packed-bed CLC power plant with coal syngas. Int J Greenh Gas Con 2015; 36, 34-50.

[37]. Fernández JR, Alarcón JM, Abanades JC. Investigation of a fixed-bed reactor for the calcination of CaCO3 by the simultaneous reduction of CuO with a fuel gas. Ind Eng Chem Res 2016; 55, 5128-32.

[38]. Alarcón JM, Fernández JR, Abanades JC. Study of a Cu-CuO chemical loop for the calcination of CaCO3 in a fixed bed reactor. Chem Eng J 2017; 325, 208-20

[39]. Dissanayake D, Rosynek MP, Kharas KC, Lunsford JH. Partial oxidation of methane to carbon monoxide and hydrogen over a Ni/Al2O3 catalyst. J Catal 1991; 132, 117-27.

[40]. Fernández JR, Abanades JC. Conceptual design of a Ni-based chemical looping combustion process using fixed-beds. Appl Energ 2014; 135, 309-19.

[41]. Navarro, RM, Peña, MA, Fierro, JLG. Hydrogen production reactions from carbon feedstocks: fossil fuels and biomass. Chem Rev 2007; 107, 3952.

[42]. Noorman S, Gallucci F, van Sint Annaland M, Kuipers H. Experimental investigation of a CuO/Al2O3 oxygen carrier for chemical-looping combustion. Ind Eng Chem Res 2010; 49, 9720-28.

[43]. Hamers HP, Gallucci F, Cobden PD, Kimball E, van Sint Annaland M. CLC in packed beds using syngas and Cu/Al2O3: Model description and experimental validation. Appl Energ 2014; 119, 163-72.

[44]. Fernández JR, Abanades JC. Optimized design and operation strategy of a Ca-Cu chemical looping process for hydrogen production. Chem Eng Sci 2017; 166, 144-60.

[45]. Jerndal E, Mattisson T, Lyngfelt A Thermal Analysis of chemical-looping combustion. Chem Eng Res Des 2006; 84, 795–806

[46]. Martínez I, Romano MC, Fernández JR, Chiesa P, Murillo R, Abanades JC. Process design of a hydrogen production plant from natural gas with CO_2 capture based on a novel Ca/Cu chemical loop. Appl Energ 2014; 114, 192-208.

[47]. Abanades JC, Rubin ES, Mazzotti M, Herzog HJ. On the climate change mitigation potential of CO_2 conversion to fuels. Energ Environ Sci 2017; 10(12), 2491-99.

[48]. Jonshagen K, Sipocz N, Genrup M. A Novel Approach of Retrofitting a Combined Cycle With Post Combustion CO_2 Capture. J Eng Gas Turb Power 2011; 133, 1-7.

[49]. van Selow ER, Cobden PD, van den Brink RW, Hufton JR, Wright A. Performance of sorption-enhanced water-gas shift as a pre-combustion CO_2 capture technology. Ener Proc 2009; 1, 689-96.

[50]. Wright AD, White V, Hufton JR, Quinn R, Cobden PD, van Selow ER. CAESAR: Development of a SEWGS model for IGCC. Ener Proc 2011; 4, 1147-54.

[51]. Martínez I, Murillo R, Grasa G, Fernández JR, Abanades JC. Integrated combined cycle from natural gas with CO_2 capture using a Ca–Cu chemical loop. AIChE J 2013; 59, 2780-94.

[52]. Romano MC, Chiesa P, Lozza G, Pre-combustion CO_2 capture from natural gas power plants, with ATR and MDEA processes, Int J Greenh Gas Con 2010; 4, 785-97.

[53]. Martinez I, Romano MC, Chiesa P, Grasa G, Murillo R, Hydrogen production through sorption enhanced steam reforming of natural gas: Thermodynamic plant assessment, Int J Hydrogen Energy 2013; 38, 15180-99.

[54]. Cloete S, Tobiesen A, Morud J, Romano MC, Chiesa P, Giuffrida A, Larring Y, Economic assessment of chemical looping oxygen production and chemical looping combustion in integrated gasification combined cycles, Int J Greenh Gas Con 2018; 78, 354-363.

[55]. Martinez I, Martini M, Riva L, Gallucci F, van Sint Annaland M, Romano MC, Techno-economic analysis of a natural gas combined cycle integrated with a Ca-Cu looping process for low CO_2 emission power production, Int J Greenh Gas Con 2019; 78, 354-363.